

UniCon: Unidirectional Split Learning with Contrastive Loss for Visual Question Answering

Yuwei Sun^{1,2} Hideya Ochiai¹

¹The University of Tokyo ²RIKEN

ywsun@g.ecc.u-tokyo.ac.jp, ochiai@g.ecc.u-tokyo.ac.jp

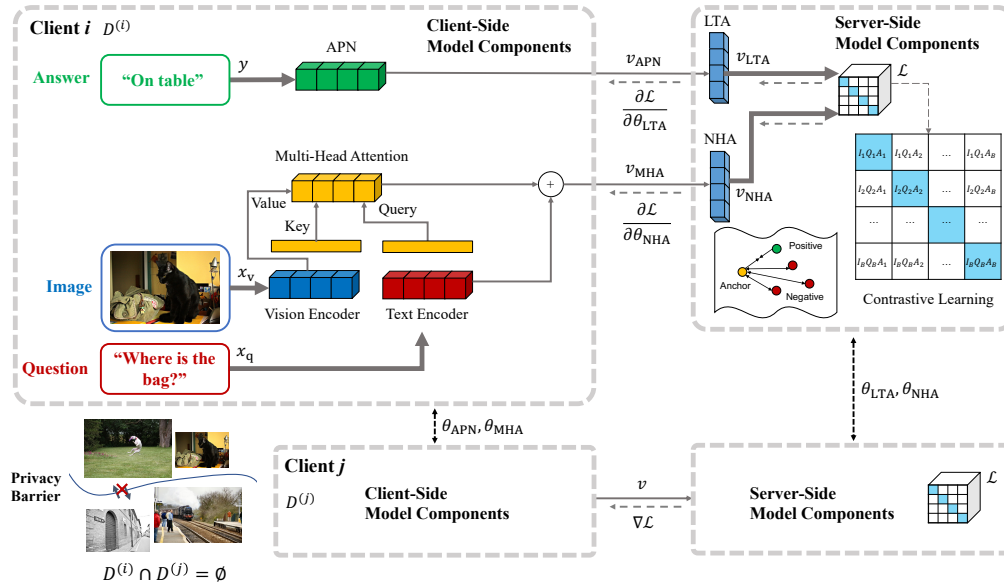


Figure 1: UniCon for confidential visual question answering consists of three main components: cross-modal representation learning (multi-head attention), an answer projection network (APN) for semantic understanding of answers, and two adapter networks (LTA and NHA) for contrastive learning of different model component outputs. UniCon learns refined representations from different client data while maintaining their privacy.

ABSTRACT

Visual Question Answering (VQA) using multi-modal data facilitates real-life applications, such as home robots and medical diagnoses. However, one significant challenge is to design a robust learning method for various client tasks. One critical aspect is to ensure privacy, as client data sharing is limited due to confidentiality concerns. This work focuses on addressing the issue of confidentiality constraints in multi-client VQA tasks and limited labeled training data of clients. We propose the **Unidirectional Split Learning with Contrastive Loss (UniCon)** method to overcome these limitations. The proposed method trains a global model on the entire data distribution of different clients, learning refined cross-modal representations through model sharing. Privacy is ensured

by utilizing a split learning architecture in which a complete model is partitioned into two components for independent training. Moreover, recent self-supervised learning techniques were found to be highly compatible with split learning. This combination allows for rapid learning of a classification task without labeled data. Furthermore, UniCon integrates knowledge from various local tasks, improving knowledge sharing efficiency. Comprehensive experiments were conducted on the VQA-v2 dataset using five state-of-the-art VQA models, demonstrating the effectiveness of UniCon. The best-performing model achieved a competitive accuracy of 49.89%. UniCon provides a promising solution to tackle VQA tasks in a distributed data silo setting while preserving client privacy.

KEYWORDS

self-supervised, split learning, privacy, visual question answering

ACM Reference Format:

Yuwei Sun^{1,2} Hideya Ochiai¹, ¹The University of Tokyo ²RIKEN, ywsun@g.ecc.u-tokyo.ac.jp, ochiai@g.ecc.u-tokyo.ac.jp . 2023. UniCon: Unidirectional Split Learning with Contrastive Loss for Visual Question Answering. In *Proceedings of arXiv preprint (Conference'23)*. ACM, New York, NY, USA, 10 pages. <https://doi.org/10.1145/nmnnnnn.nmnnnnn>

Permission to make digital or hard copies of all or part of this work for personal or classroom use is granted without fee provided that copies are not made or distributed for profit or commercial advantage and that copies bear this notice and the full citation on the first page. Copyrights for components of this work owned by others than ACM must be honored. Abstracting with credit is permitted. To copy otherwise, or republish, to post on servers or to redistribute to lists, requires prior specific permission and/or a fee. Request permissions from permissions@acm.org.
Conference'23, Apr 2023, arXiv preprint

© 2023 Association for Computing Machinery.
ACM ISBN 978-x-xxxx-xxxx-x/YY/MM...\$15.00
<https://doi.org/10.1145/nmnnnnn.nmnnnnn>

1 INTRODUCTION

The deployment of multi-modal models in safety-critical applications, such as personal robots and healthcare, requires addressing various model vulnerabilities and robust architecture design. Numerous studies have highlighted the privacy concerns of large models like GPT-4 [27], due to the vast amount of user data it collects. This centralized approach increases the risk of data breaches or misuse of user data. However, few studies have focused on practical privacy-preserving architecture design for these models. There is a growing need for personal models that can operate at the edge, due to data confidentiality.

To bridge the gap between the need for large-scale training in multi-modal models and the constraint of data confidentiality, the privacy in multimodal systems and applications should be addressed properly. The development of privacy-preserving multimodal models could enable the effective engagement of users while preserving their privacy, enhancing the user experience in applications that require privacy preservation.

To address this problem, we study decentralized machine learning methods [35] for a specific multi-modal task, i.e., Visual Question Answering (VQA). Training a VQA model usually requires a large amount of data in both texts and images that encompass a wide range of personal interests. A privacy-preserving VQA framework has not been studied until recently. Decentralized machine learning approaches such as federated learning (FL) [25], are used to facilitate the distributed training of models across different data silos without compromising the raw data. For instance, connected home robots could learn to better generalize to new dialogues by transferring knowledge from other robots through parameters sharing, without disclosing sensitive personal data of each user.

Previous studies have shown that although federated learning (FL) can protect data privacy, it fails to ensure model privacy as the shared parameters of a user model can reveal the data used for training via an information stealing attack [14] or enable a Trojan attack targeting the model architecture [24]. This is because FL involves sending model updates to a central server for aggregation, which can be vulnerable to attacks that expose sensitive information about the model. In contrast, split learning prevents access to the raw data or model architecture by keeping the partial model parameters on the local device [36].

In this work, we propose a novel privacy-preserving split learning framework for VQA that addresses challenges related to protecting training data and model architecture. Moreover, a consolidation with self-supervised learning shows particularly useful to tackle unlabeled data at the edge. Our proposed method, **Unidirectional Split Learning with Contrastive Loss (UniCon)**, refines cross-modal representations from the question-image-answer triplets of different users (Fig. 1). By keeping partial model parameters on local devices, this method facilitates model training on distributed data silos while preserving privacy.

The main contributions of this work are as follows:

- 1) This work is the first study of using Split Learning to ensure model privacy in VQA.
- 2) We propose a new contrastive loss-based split learning framework, called Unidirectional Split Learning with Contrastive Loss

(UniCon), which overcomes the inefficiency of bidirectional representations and gradients sharing in classical Split Learning.

3) This study demonstrates UniCon’s ability to handle unlabeled data at the edge by leveraging self-supervised learning. UniCon aligns different modality representations by encouraging similarity between relevant model component outputs and discouraging similarity between irrelevant component outputs in Split Learning.

4) An in-depth evaluation on the VQA-v2 dataset was conducted using seven state-of-the-art models and their variants, with UniCon achieving competitive performance compared to centralized VQA models while maintaining a much higher level of privacy protection.

2 RELATED WORK

2.1 Visual Question Answering

In recent years, Multimodal machine learning (MMML) [3, 9, 31–33] has been intensively studied with significant progress in understanding and reasoning across different modalities of information in the real world. A specific task within MMML is Visual Question Answering (VQA), which involves answering natural language questions based on the contents of a presented image. VQA is actively studied [4, 16, 42] with much progress in recent years coming from the use of attention mechanism [37]. Nevertheless, the vast majority of VQA studies so far rely on modality network fusion methods [17, 40] where the VQA task is considered a multi-class classification. This assumption hinders the understanding of semantic notions embedded in the natural language answers. Moreover, in practice, these studies do not touch on the privacy of VQA when using multi-modal data for training. This work aims to bridge the gap between the requirement for large-scale training data in VQA and the constraint of data confidentiality (Table 1).

In recent years, there has been an intensive focus on Multimodal machine learning (MMML) [3, 9, 31–33] with significant strides in understanding and reasoning across different modalities of information in the real world. GPT-4 [27] is a large multimodal model using images and texts as inputs to output text responses. This specific area of MMML that has gained much attention is Visual Question Answering (VQA), where a natural language question is answered based on the contents of a presented image. VQA is an active area of research [4, 16, 42], and recent progress has been made through the use of attention mechanisms [37]. However, the vast majority of VQA studies do not address the issue of privacy when training on large-scale multi-modal data and the collected instructions from human feedback [28]. This work aims to bridge the gap between the need for large-scale training in VQA and the constraint of data confidentiality, leading to a better user experience in VQA and other multimedia applications.

2.2 Decentralized Machine Learning

Decentralized Machine Learning involves methods such as Federated Learning [12, 21, 25, 34], Split Learning [36], and Swarm Learning [39]. While Federated Learning have been studied for tasks of a single modality [35], studies on multimodal models such as VQA are still limited. In particular, for the visual language grounding tasks, Liu et al. [23] proposed a Federated Learning-based VQA framework called the aimNet that acquires fine-grained representations from different clients for improved downstream tasks. However, aimNet

Methods	Shared Data	Shared Model	Learning Framework	Loss Function
MMNas [42]	✓	✓	Single fusion model	Cross entropy loss
QICE [46]	✓	✓	Single fusion model	Cross entropy loss + Contrastive loss
CLIP [9]	✓	✓	Single fusion model	Contrastive loss
aimNet [23]	×	✓	Federated Learning	Cross entropy loss
UniCon (Ours)	×	×	Unidirectional Split Learning	Contrastive loss

Table 1: Summary of existing work designed for tackling VQA tasks. Compared to the previous work, UniCon does not require sharing training data or models. This is enabled by a unidirectional split learning framework with the contrastive loss.

is a supervised learning framework that trains on the hard labels for different answers. Moreover, though aimNet does not disclose client data during training, a client’s entire model parameters need to be shared for learning better-refined representations.

Decentralized Machine Learning encompasses methods like Federated Learning (FL) [12, 21, 25, 34], Split Learning (SL) [36], and Swarm Learning [39]. These methods address privacy concerns by enabling collaborative learning without the need for centralized data storage. Multiple parties train models using their local data without sharing it, preserving data privacy and reducing the risk of data breaches. Although FL has been widely investigated for single-modality tasks [35], its application to multimodal models like VQA is still limited. A FL-based VQA framework called aimNet was proposed by Liu et al. [23], which utilizes fine-grained representations from various clients to enhance downstream tasks. However, aimNet only guaranteed the data privacy of a user. The entire user model was transmitted to the server to enhance performance by incorporating representations from multiple users. Therefore, the model privacy is not guaranteed in aimNet (as shown in Table 1). UniCon addresses the challenge of model privacy by separating the model into two parts: the first part is kept on the user’s device, while the second part is kept on a remote server. The user’s device first propagates the input data, and then sends the hidden layer activations to the server. The server computes the output using its part of the model and sends the gradient back to the user. This process guarantees privacy by not exposing either the input data or the model architecture. To the best of our knowledge, this is the first time split learning has been leveraged for VQA.

2.3 Self-Supervised Learning

The prerequisite of large-scale training tasks like VQA that requires a decent amount of labeled data can be a hindrance, as data collection and labeling processes can be time-consuming and costly. Most VQA research has focused on supervised learning using one-hot vectors of answer classes as labels [4, 16, 40]. This approach does not take into account the meaning of the answers and the semantic correlation between the multi-modal inputs and answers.

Recent studies in MML have seen a shift towards self-supervised learning (SSL) methods, particularly contrastive learning [7, 8, 18]. Contrastive learning trains a shared embedding space from unlabelled data by keeping similar sample pairs close and dissimilar pairs far apart. For example, Barlow Twins[45] learns a cross-correlation matrix by keeping representations of distorted versions of an input sample similar while minimizing redundancy between them. MoCo [13] uses InfoNCE loss [26] to match encoded queries to a dictionary of encoded keys and train a visual representation

encoder. Contrastive learning is also used to train multimodal models, such as CLIP [9], which computes a cosine similarity matrix among all possible candidates of images and texts within a batch. Question-Image Correlation Estimation (QICE) [46] trains on relevant image and question pairs in VQA datasets to alleviate the language prior problem [11]. Nevertheless, CLIP and QICE do not address privacy concerns and do not provide any guarantees regarding data or model privacy. We found that contrastive learning is a natural fit for split learning to achieve privacy-preserving SSL in VQA tasks. This approach eliminates the need for training labels and preserves the privacy of both data and the model, which could greatly enhance user experience in real-world applications.

3 METHODS

This section presents the proposed method, Unidirectional Split Learning with Contrastive Loss (UniCon), for visual question answering (VQA) tasks. First, the motivation behind this method was demonstrated, followed by a discussion of its technical underpinnings. Notably, this encompasses the split learning for VQA model privacy, the answer projection network for semantic notions understanding, and the contrastive learning architecture for the training on unlabeled user data.

3.1 Motivation

In visual question answering (VQA), training data is typically collected before model training. Methods such as federated learning improve a model’s performance while maintaining certain data confidentiality, by sharing locally trained models instead of raw data [25]. However, the model architecture and its parameters still need to be disclosed. In contrast, UniCon aligns different model components partitioned to enable training via sharing a middle layer’s activations, without revealing either the user data or the model architecture. This avoids the potential misuse of the exposed model architecture by attackers, such as mounting a Trojan attack using the revealed architecture. Furthermore, the advancement in contrastive learning has shown to be a natural fit with split learning for training upon unlabeled user data. This consolidation further enhances privacy preservation by leveraging the semantic notions of input texts instead of the finite one-hot vectors. UniCon aims to enhance user experience in applications that require privacy consideration while enabling effective engagement of different users to improve the model performance.

3.2 Split Learning for VQA

Visual Question Answering (VQA) is a task that involves answering natural language questions based on the visual content of a given

image. Typically, the VQA problem is approached as a supervised learning task with a predetermined list of C potential answer options. Let f_{MHA} be the VQA model that takes as the input the pair of an image $x_v \in \mathbb{R}^V$ and a question $x_q \in \mathbb{R}^Q$ and outputs an answer $\hat{y} \in \{y_1, y_2, \dots, y_C\}$ where $y_c \in \mathbb{R}^A$. A VQA model aims to predict the correct answer y given the input pair $(x_v, x_q) \in D$ where D is the dataset. $\hat{y} = \arg \max_y p(y|x_v, x_q; f_{\text{MHA}})$ where $p(\cdot|\cdot)$ is the conditional probability.

This work considers a diverse set of VQA models that are based on the attention mechanism [38] (Section 4.1.2). At its simplest form, the attention mechanism in a VQA model can be formulated as follows. Each head of a multi-head attention maps a query and a set of key-value pairs to an output. In particular, in a single head i , the output is calculated as a weighted sum of values based on the attention scores, which are computed by a function of the query with the corresponding key. Let $W^{\text{text}} \in \mathbb{R}^{Q \times M}$ be an encoder to process the text input x_q (such as LSTM [15] and Transformer [38]), and $W^{\text{vision}} \in \mathbb{R}^{V \times P}$ be an encoder to process the vision input x_v (such as CNN [20] and MLP [6]). The linearly projected output of the text encoder is used as a query $Q \in \mathbb{R}^d \leftarrow W^{Q_i} W^{\text{text}} x_q$, which is compared with that of the vision encoder which serves as the key $K \in \mathbb{R}^d \leftarrow W^{K_i} W^{\text{vision}} x_v$. Here, $W^Q \in \mathbb{R}^{M \times d}$ and $W^K \in \mathbb{R}^{P \times d}$ are linear transformations for the query and key. Then, the weighted sum of values $V \in \mathbb{R}^P \leftarrow W^{\text{vision}} x_v$ is computed with the attention scores as the weights, which are determined using the dot product of the query and key. Finally, the outputs of different heads are concatenated and projected. The attention layers are updated such that weights are put on the visual regions that are more relevant to the question. The multi-head attention (MHA) that utilizes the vision and text inputs in VQA is formulated as follows

$$h^i(x_v, x_q) = \text{softmax}\left(\frac{W^{Q_i} W^{\text{text}} x_q (W^{K_i} W^{\text{vision}} x_v)^T}{\sqrt{d}}\right) W^{\text{vision}} x_v,$$

$$\text{Multi-head}(x_v, x_q) = \text{Concat}(h^1, \dots, h^H) W^O,$$

where W^O is a linear transformation for outputs, and H is the number of attention heads.

Split Learning (SL) divides the complete model into different parts and trains a global model via interactive forward activation and backward gradient sharing. Following [36], this work employs SL without label sharing that wraps the model on the server around the end layer and sends the layer output back to a client (Fig. 2.a). This architecture guarantees the data confidentiality of a client since both input data and labels are not shared during training. Additionally, when integrated with contrastive learning, this architecture could yield further advantages, which is elaborated upon in the subsequent section. A complete model is split into three components in SL, i.e., a global component f_g and two client components $\{f_{c,1}, f_{c,2}\}$. Assuming K clients, each client has its own dataset $D^{(k)}$, which consists of $N^{(k)}$ samples, represented as $\{(x_{v,j}, x_{q,j}, y_j)\}_{j=1}^{N^{(k)}}$. Here, $\cup_{k=1}^K D^{(k)} = D$, $D^{(i)} \cap D^{(j)} = \emptyset, \forall i \neq j$, and $\sum_{k=1}^K N^{(k)} = N$, where N is the sample size. The components of clients share the same architecture, and data sharing is not possible due to data confidentiality. Refer to Appendix 2 for further details on the algorithm.

3.3 Unidirectional Split Learning with Contrastive Loss

A major challenge in VQA is the reliance on supervised learning, where the semantic understanding of answers is often misaligned with the inputs, reducing the generality of the trained models to unseen samples. The most majority of standard VQA datasets like VQA-v2 usually annotate the image and question pairs with just a numeric id of the answer label and contain a file mapping these ids back to answers in English [9]. Due to the lack of contexts and semantic notions, it is usually difficult for the text encoder to disentangle features that are relevant to the input. Previous work has shown the plausible usages of Contrastive Learning to learn refined cross-modal representations from raw image and text inputs [9, 33]. To this end, we propose using a contrastive loss in conventional Split Learning to improve the correlation between visual and language contents of clients, improving the global model without relying on numeric labels. This approach provides more relaxation to the model training while maintaining a user's privacy.

3.3.1 Answer Projection Network and Adapter Networks. Supervised VQA models [4, 16, 40] using numeric labels do not take into account the semantic notions of different answers. By contrast, this work proposes an Answer Projection Network (APN) f_{APN} that projects a lexical answer y into a feature vector $v_{\text{APN}} \in \mathbb{R}^S$. In particular, APN employs a text preprocessing module using a pre-trained word embedding called GloVe [30], to transform the question into a fixed-size vector representation. The resulting vector is then passed through a linear projection layer.

Two adapter networks are employed to project the outputs from client-side model components into a shared projection space. In particular, a nonlinear projection head on more complex representations could improve the performance while it is not beneficial for tackling simpler modality representations [3, 7]. The VQA model f_{MHA} 's output layer is replaced with the Nonlinear Head Adapter (NHA) network f_{NHA} that projects the high-level cross-modal representations from the layer before the output layer into the shared projection space $v_{\text{NHA}} \in \mathbb{R}^S$. The Linear Tail Adapter (LTA) is devised to project the low-level representations v_{APN} of APN into the shared projection space $v_{\text{LTA}} \in \mathbb{R}^S$. Note that v_{LTA} and v_{NHA} have the same dimension of S . Refer to Section 4.2 for the detailed architecture of APN, NHA, and LTA.

3.3.2 Learning with the Information Noise Contrastive Estimation loss. The Information Noise Contrastive Estimation (InfoNCE) loss is used for contrastive learning [26] in this work, which is a self-supervised learning approach that learns representations by contrasting similar and dissimilar pairs of data points. Notably, UniCon employs the NHA and LTA outputs of the same input triplets within one training batch as positive pairs. $\{(v_{\text{NHA},j}, v_{\text{LTA},j})\}_{j=1}^B$ where B is the sample size of the training batch. In contrast, given a NHA output $v_{\text{NHA},i}$, any irrelevant LTA outputs $\{v_{\text{LTA},j}|j \neq i\}_{j=1}^B$ are employed as the negative keys of the NHA output. The dot product similarity is used as a measure of similarity between the two representations. Then, the model is trained by aligning between the component outputs of positive pairs while discouraging the similarity between the negative pairs (Fig. 3). The loss \mathcal{L} can be formulated as follows

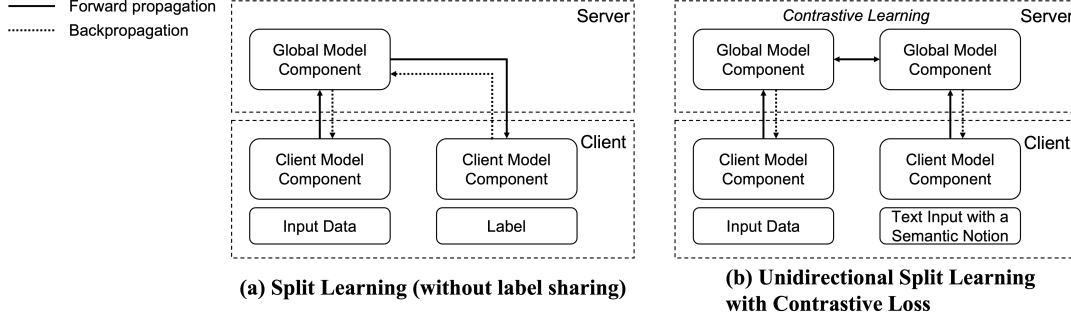


Figure 2: Conventional Split Learning vs. UniCon: Split Learning (left) utilizes numeric one-hot vectors of answer labels for model training, based on a bidirectional process that requires sequential processing of components causing longer waiting time. In contrast, UniCon (right) employs lexical semantic notions of answer texts and a unidirectional process that enables concurrent processing of model components.

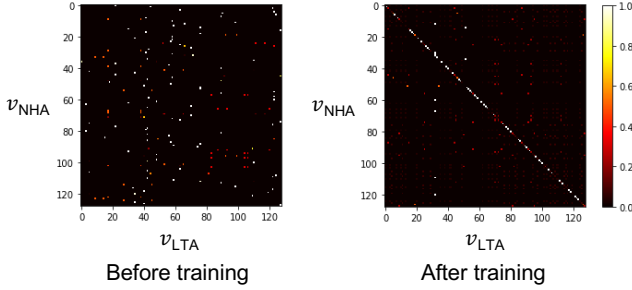


Figure 3: Measured dot product similarity between any two representations in one batch before and after training with UniCon. The similarity scores are optimized such that the representations of positive pairs have a higher score while that of the negative pairs have a lower score.

$$\mathcal{L} = - \sum_{i=1}^B \log \frac{\exp(v_{\text{NHA},i} \cdot v_{\text{LTA},i}/\tau)}{\sum_{j=1}^B \mathbb{1}_{[j \neq i]} \exp(v_{\text{NHA},i} \cdot v_{\text{LTA},j}/\tau)}, \quad (1)$$

where τ is the temperature parameter to ensure the output is appropriately scaled to the data distribution, and $\mathbb{1}_{[j \neq i]}$ is an indicator function: 1 if $j \neq i$, 0 otherwise.

Moreover, the information flow between a client and the server is bidirectional in conventional SL (Fig. 2.a), where components process data in subsequent which largely increases the waiting time of a client. Contrastive learning adapts the conventional bidirectional process for a novel unidirectional process, which enables parallel processing of model components. In this architecture, layer activations are sent from clients to the server, and gradients are sent from the server to clients. As a result, clients can utilize all their local components concurrently while computing activations or gradients, without waiting for the computation of the next component. This training process leads to significant improvements in user experience and the efficiency of the model (Fig. 2.b).

3.3.3 Parameter Aggregation. Parameter aggregation of models trained by different clients aims to improve the generality of the global model to unseen samples. This is enabled by aggregating the update gradients of different components after each epoch's

training. To protect client model privacy, a dual-server model parameter aggregation approach that leverages a second auxiliary server to aggregate the client components (APN and MHA) is devised, since sending the client components to the main server for aggregation would violate the model privacy guarantee of UniCon. The global components (NHA and LTA) are aggregated on the main server. The parameter aggregation based on an averaging method is formulated as follows

To improve the generalization of the global model to unseen samples, the update gradients of different components are aggregated after each epoch's training. To further preserve the privacy of client models during aggregation, a dual-server aggregation approach is devised, which involves a second auxiliary server to aggregate the client components (APN and MHA). Because sending these components to the main server (parameter server) would violate the guarantee of model privacy. The global components (NHA and LTA) are aggregated on the main server, and the aggregation process employs an averaging method, as formulated below:

$$\delta\theta_t = \frac{1}{K} \sum_{k \in \{1,2,\dots,K\}} (\theta_{t+1}^{(k)} - \theta_t^{(k)}), \quad (2)$$

where θ is the parameters of a model component from $\{\theta_{\text{APN}}, \theta_{\text{MHA}}, \theta_{\text{NHA}}, \theta_{\text{LTA}}\}$.

The full details of the UniCon algorithm are presented in Algorithm 1. UniCon proceeds by iterating the following steps: 1) each client forward propagates the triplet inputs (i.e., images, questions, and answers) using APN and MHA and sends the output activations of these components to the parameter server (PS), 2) the PS takes as input the client-side activations and computes the contrastive loss using LTA and NHA, 3) the PS computes the gradients to update LTA and NHA and sends the gradients back to the client for the update of APN and MHA, and 4) model parameter aggregation is performed based on the dual-server approach. This process is repeated until a given training goal is achieved.

4 EXPERIMENTS

In this section, a detailed description of the datasets, model architectures, and metrics used in the experiments is provided. Then,

Algorithm 1 Unidirectional Split Learning with Contrastive Loss

```

1:  $T$ : number of split learning rounds
2:  $E$ : number of local epochs
3:  $\eta$ : learning rate
4: for each round  $t = 1, 2, \dots, T$  do
5:   for each client  $k \in \{1, 2, \dots, K\}$  in parallel do
6:     for  $\theta \in \{\theta_{\text{APN}}, \theta_{\text{MHA}}, \theta_{\text{NHA}}, \theta_{\text{LTA}}\}$  do
7:        $\theta_t^{(k)} \leftarrow \theta_t$ 
8:     end for
9:     for each local epoch  $e = 1, 2, \dots, E$  do
10:       $v_{\text{MHA},t,e}^{(k)} = f_{\text{MHA}}(\theta_{\text{MHA},t,e}^{(k)}, (x_v^{(k)}, X_q^{(k)}))$ 
11:       $v_{\text{APN},t,e}^{(k)} = f_{\text{APN}}(\theta_{\text{APN},t,e}^{(k)}, Y^{(k)})$ 
12:       $\delta_{\text{NHA},e}^{(k)}, \delta_{\text{LTA},e}^{(k)} = \text{Server}(v_{\text{MHA},t,e}^{(k)}, v_{\text{APN},t,e}^{(k)})$ 
13:       $\theta_{\text{MHA},t,e+1}^{(k)} \leftarrow \theta_{\text{MHA},t,e}^{(k)} - \eta \cdot \frac{\partial \delta_{\text{NHA},e}^{(k)}}{\partial \theta_{\text{MHA},t,e}^{(k)}}$ 
14:       $\theta_{\text{APN},t,e+1}^{(k)} \leftarrow \theta_{\text{APN},t,e}^{(k)} - \eta \cdot \frac{\partial \delta_{\text{LTA},e}^{(k)}}{\partial \theta_{\text{APN},t,e}^{(k)}}$ 
15:    end for
16:  end for
17:  for  $\theta \in \{\theta_{\text{APN}}, \theta_{\text{MHA}}, \theta_{\text{NHA}}, \theta_{\text{LTA}}\}$  do
18:     $\theta_{t+1} = \frac{1}{K} \sum_{k \in K} \theta_{t,E+1}^{(k)}$ 
19:  end for
20: end for
21:
22: function  $\text{Server}(v_{\text{MHA},t,e}^{(k)}, v_{\text{APN},t,e}^{(k)})$ 
23:  $v_{\text{NHA},t,e}^{(k)} \leftarrow f_{\text{NHA}}(v_{\text{MHA},t,e}^{(k)})$ 
24:  $v_{\text{LTA},t,e}^{(k)} \leftarrow f_{\text{LTA}}(v_{\text{APN},t,e}^{(k)})$ 
25:  $\mathcal{L} = - \sum_{i=1}^B \log \frac{\exp(v_{\text{NHA},i} \cdot v_{\text{LTA},i} / \tau)}{\sum_{j=1}^B \mathbb{1}_{[j \neq i]} \exp(v_{\text{NHA},i} \cdot v_{\text{LTA},j} / \tau)}$ 
26:  $\delta_{\text{NHA},e}^{(k)} = \frac{\partial \mathcal{L}}{\partial v_{\text{NHA},t,e}^{(k)}}$ 
27:  $\delta_{\text{LTA},e}^{(k)} = \frac{\partial \mathcal{L}}{\partial v_{\text{LTA},t,e}^{(k)}}$ 
28:  $\theta_{\text{NHA},t,e+1}^{(k)} \leftarrow \theta_{\text{NHA},t,e}^{(k)} - \eta \cdot \delta_{\text{NHA},e}^{(k)}$ 
29:  $\theta_{\text{LTA},t,e+1}^{(k)} \leftarrow \theta_{\text{LTA},t,e}^{(k)} - \eta \cdot \delta_{\text{LTA},e}^{(k)}$ 
30: return  $\delta_{\text{NHA},e}^{(k)}, \delta_{\text{LTA},e}^{(k)}$  to client  $k$ 

```

the performance of UniCon is compared with a supervised method and a contrastive learning-based method, both of which are centralized without privacy guarantees. The empirical results on five different state-of-the-art (SOTA) VQA models and their variants are demonstrated, followed by a thorough discussion.

4.1 Dataset and Models

4.1.1 Dataset. Our method was evaluated on the benchmark dataset VQA-v2 [2] with varying partitioning configurations for UniCon. VQA-v2 covers 82.8k images and 443.8k questions for training and 40.5k images and 214.4k questions for validation. The images are from the COCO dataset [22] with a size of 640×480. The results on the validation splits were reported.

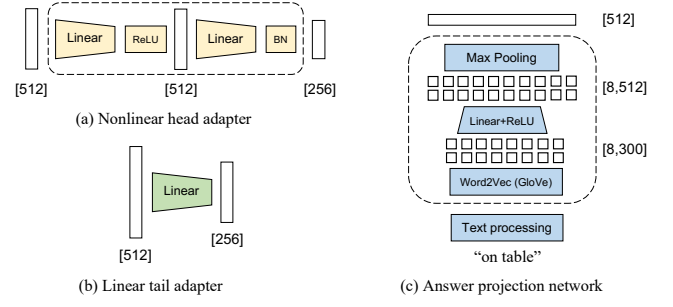


Figure 4: The model architectures of the nonlinear head adapter (NHA), the linear tail adapter (LTA), and the answer projection network (APN). The number of neurons in each layer is indicated by the numbers within square brackets.

4.1.2 VQA Models. The following SOTA VQA models and their variants with different model sizes were studied and tailored for contrastive learning and UniCon: (1) Multi-modal Factorized Bilinear (MFB) [44] combines multi-modal features using an end-to-end network architecture to jointly learn the image and question attention, (2) Bottom-Up and Top-Down attention mechanism (BUTD) [4] enables attention to be calculated at the level of objects and other salient image regions. The bottom-up mechanism based on Faster R-CNN proposes image regions, while the top-down mechanism determines feature weightings, (3) Bilinear Attention Networks (BAN) [16] considers bilinear interactions among two groups of input channels and extracts the joint representations for each pair of channels, (4) Multimodal neural architecture search (MMNas) [42] uses a gradient-based algorithm to learn the optimal architecture, and (5) Modular Co-Attention Network (MCAN) [43] consists of Modular Co-Attention layers cascaded in depth where each layer models both the self-attention and the guided-attention of the input.

4.1.3 Implementation Details. The proposed privacy-preserving method is compatible with different VQA models. The evaluation was conducted on three different settings for each model: centralized supervised learning, centralized contrastive learning, and UniCon for decentralized learning on client datasets. The model performance was evaluated with three different seeds and the mean was reported. The VQA models were implemented using PyTorch with their default author-recommended hyperparameters. The experiments were conducted on four NVIDIA A100 GPUs with 40GB memory, and the code will be made publicly available.

4.2 Architecture and Hyperparameters

The following architectures were employed for the nonlinear head adapter (NHA), the linear tail adapter (LTA), and the answer projection network (APN), respectively (Fig. 4). For APN, the GloVe [30] trained on Common Crawl was used to convert the answer texts with a maximum word of eight into $\mathbb{R}^{8 \times 300}$, padded with zero vectors. Then, a fully-connected (FC) layer followed by the ReLU activation projected the representations into $\mathbb{R}^{8 \times 512}$. Finally, a Max Pooling layer was employed producing 512-dimension vectors. Moreover, for LTA, a FC layer projected the representations received from each client to the shared space with a dimension of

VQA Models	Supervised learning-based VQA (%)			
	Overall	Yes/No	Number	Other
BAN [16]	65.86	83.53	46.36	57.56
BUTD [4]	63.84	81.40	43.81	55.78
MFB [44]	65.35	83.23	45.31	57.05
MCAN-s [43]	67.17	84.82	49.31	58.48
MCAN-l [43]	67.50	85.14	49.66	58.80
MMNas-s [42]	67.79	85.02	52.25	58.80
MMNas-l [42]	67.98	85.22	52.04	59.09

Table 2: Performance upper bounds of VQA task using supervised learning-based methods for different models.

256. For NHA, a FC layer projected the representations to a dimension of 512 followed by ReLU activation function. Then, another fully connected layer was used to further project the output to a dimension of 256 followed by batch normalization.

Furthermore, the selection of hyperparameters was performed through the grid search. A batch size of 128, a total epoch of 20 (693.4k steps), Adam ($\beta_1 = 0.9$, $\beta_2 = 0.999$, $\epsilon = 10^{-8}$), and a linear warmup of 10K steps with an initial learning rate of 0.0001 and a decay rate of 0.2 at the epoch 10 and 15, were employed. For the InfoNCE loss, a temperature of 0.07 was employed as in [3, 29].

4.3 Proposed Metric

Measuring the accuracy of UniCon is challenging due to the lack of a discriminative model that can infer the class of the input. UniCon embeds the semantic meanings of answers using Glove embeddings in the Answer Projection Network (APN), converting text to numerical vectors based on semantic text distances. If two answers are semantically similar, then the learned representations of APN will also have a high similarity. To evaluate the prediction accuracy, the product similarity is measured between the cross-modal representations v_{NHA} of an input pair (x_v, x_q) from the hold-out validation dataset D_{val} and the representations $v_{\text{LTA},c}$ of C answer options $y_c \in \{y_1, y_2, \dots, y_C\}$. $v_{\text{LTA},c}$ denotes the representation of answer option y_c . Then, the answer with the highest similarity with the input is selected as the predicted answer \hat{y} . There also exist studies reporting the average accuracy of different batches, i.e., measuring the similarity scores for samples from the same batch. However, such a metric can easily produce a much higher accuracy compared to the metric using all answer options. Therefore, the similarity scores based on all answer options are employed as the metric, which is formulated as follows

$$\text{ValAcc} = \frac{\sum_{(x_v, x_q, y) \in D_{\text{val}}} \mathbb{1}\{\arg \max_c (v_{\text{NHA}} \cdot v_{\text{LTA},c}) = y\}}{|D_{\text{val}}|}. \quad (3)$$

4.4 Empirical Results

In this section, the effectiveness of the contrastive learning approach in VQA was evaluated and compared with the supervised method. Then, we conducted experiments on UniCon that allows for decentralized training while ensuring both data and model privacy. The comparison between the contrastive learning approach and UniCon provided insights into the potential benefits of UniCon in situations where privacy is critical.

4.4.1 Supervised and Contrastive Learning-Based Methods for VQA.

Extensive experiments based on the five state-of-the-art VQA models above were conducted. In particular, for MMNas and MCAN, we further considered the effectiveness of different model complexities using MMNas-small (MMNas-s) and MMNas-large (MMNas-l), and MCAN-small (MCAN-s) and MCAN-large (MCAN-l), which resulted in a total of seven different models. The detailed architecture designs of these models followed the settings in previous works [42, 43]. Moreover, the proposed method’s performance was evaluated based on Eq. 3. For each triplet in the validation set, we input the image and question pair to the model, then use the output representation of the nonlinear head adapter to measure the similarity scores with the representations from the linear tail adapter of all the answer options. The prediction is made based on the answer with the highest similarity score (Fig. 5).

Table 2 presents the upper bounds achieved by different VQA models using supervised methods, which serve as a reference for evaluating the proposed privacy-preserving methods. By comparing with the upper bounds, we can gain insights into the tradeoff between performance and privacy. For the experimental settings of the supervised methods, refer to [41]. In comparison, Table 3 shows the evaluation results of the contrastive learning-based method, which can be adapted to different VQA models with a performance tradeoff compared to the supervised approach. This tradeoff, as also observed in previous studies [9], becomes more apparent when the label space is very large, especially for the 3048-dimension label space in VQA-v2 tasks considered in this work. However, the benefit of this contrastive learning-based approach is twofold: it does not require manual labeling of answer data and can use the raw text input instead, and its combination with split learning is a natural fit for a better user experience in decentralized learning. Furthermore, by comparing the results of contrastive learning on different VQA models, several architectures outperformed the others. BAN showed the worst performance, particularly in the task of counting numbers (Number). MMNas-l showed the best overall performance of 53.82%, outperforming the other models for the tasks of counting numbers and answering the image contents (Other). MCAN-l performed the best in the Yes/No questions.

4.4.2 UniCon for Privacy-Preserving Split Learning in VQA.

To evaluate the efficacy of UniCon, the training set was randomly divided into two subsets, which were employed as the local datasets of two clients. The clients shared the same model component architecture but were not permitted to share data due to confidentiality concerns. The performance was evaluated on the aggregated model after each round’s parameter aggregation. The numerical results in Table 3 show that UniCon improved the model performance by leveraging other clients’ knowledge of different local tasks, while safeguarding the privacy of each client regarding their data and model architecture.

The results demonstrate that while there exists a trade-off between model performance and using UniCon for confidentiality, UniCon enables clients to train over the entire data distribution, improving the model performance in situations where privacy is a concern. Moreover, the results show that MMNas-l outperformed the other models overall, while MCAN-l performed the best in the Yes/No questions. Compared to the overall accuracy of 53.82% of the

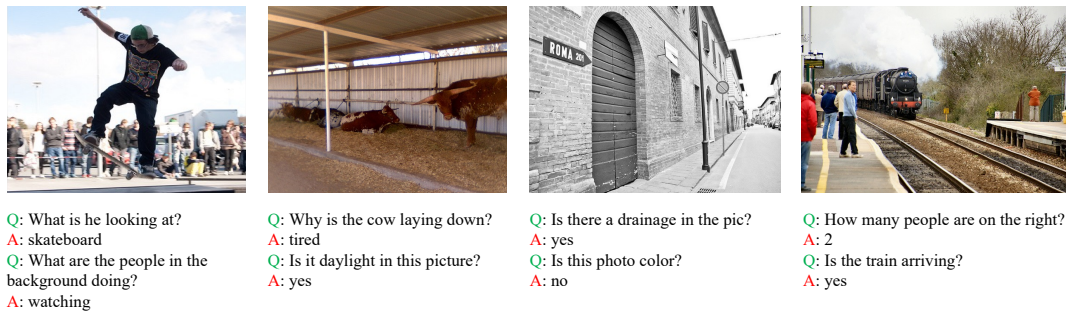


Figure 5: Examples of the visual question answering tasks that encompass a range of question types and scenes.

VQA Models	Contrastive learning-based VQA(%)				UniCon(%)			
	Overall	Yes/No	Number	Other	Overall	Yes/No	Number	Other
BAN [16]	36.23	66.90	12.71	19.11	35.11	63.84	11.06	19.61
BUTD [4]	45.08	75.82	29.27	25.86	40.96	66.98	13.34	28.74
MFB [44]	46.98	73.95	32.81	30.20	42.43	68.65	23.33	27.52
MCAN-s [43]	53.18	81.06	41.95	34.93	48.42	74.93	30.88	32.89
MCAN-l [43]	53.32	81.21	42.66	34.90	48.44	77.44	30.72	32.01
MMNas-s [42]	51.54	78.06	39.76	34.46	45.14	70.55	28.04	30.33
MMNas-l [42]	53.82	80.06	42.86	36.75	49.89	74.85	36.88	34.33

Table 3: The comparison between the contrastive learning-based method (centralized) and UniCon (decentralized privacy-preserving VQA). Compared to the supervised method, the contrastive learning-based VQA was trained on unlabeled image and text data. UniCon considered two clients, where each client trains a contrastive learning-based model on their own set of unlabeled data. Then, they collaborate to train a global model over the entire data distribution using split learning.

MMNas-l model trained over the entire dataset, UniCon obtained an accuracy of 49.89%, which is slightly lower than the accuracy of the centralized method. However, this difference in accuracy is reasonable considering the benefits in preserving privacy.

A statistical paired t-test with two-tails [19] was performed to compare the results in Table 3. With a significance level of 0.05 and a degree of freedom $n - 1 = 6$ where n is the number of models, the p -value of the results was 2.477. Based on the guarantee [19] of the paired t-test, since $t = 1.357$ falls within the range of the p -value $[-2.477, 2.477]$, there is no significant difference in the accuracy between the two methods. UniCon achieved competitive performance on VQA while maintaining the privacy of users.

4.4.3 Robustness to Trojan Attacks. Trojan attacks pose a significant threat to the security of machine learning models, and it is important to evaluate the robustness of UniCon against such attacks. In particular, we studied the Trojan attacks that embed a trigger or a backdoor pattern in the training data, causing the model to behave maliciously and output an incorrect prediction other than the label class (untargeted attack), when triggered by a specific input. We implemented the attack as described in [24] and evaluated the robustness of UniCon against such attacks. The experiments were conducted on the VQA-v2 dataset using different model architectures and the MCAN-s [43] VQA model. The empirical results show that UniCon maintains stronger robustness against such attacks (Fig. 6), demonstrating its potential for secure deployment in real-world scenarios. Nevertheless, further research would be needed in the future to investigate and improve the resilience of UniCon against more sophisticated Trojan attacks.

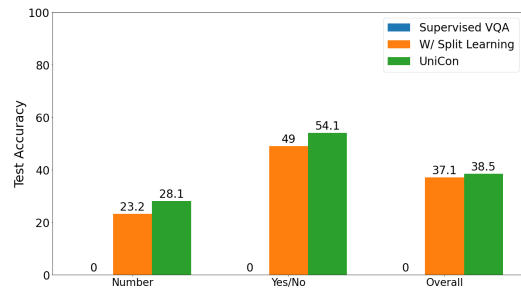


Figure 6: VQA tasks performance under the Trojan attack.

5 CONCLUSION

We proposed a novel privacy-preserving learning framework called UniCon, for visual question answering (VQA) tasks. UniCon effectively learns refined cross-modal representations by aligning different model components and aggregating knowledge from different clients. Extensive experiments on the VQA-v2 dataset demonstrated the effectiveness of UniCon across different VQA models, while maintaining the user privacy. In the future, we aim to further investigate the robustness of UniCon against adversarial attacks and leverage differential privacy [1] to safeguard communication between the components. In addition, the prompt engineering [10] would expand the list of possible answers, improving the performance of contrastive learning. This would help mitigate the trade-off between performance and privacy. We hope that this work will motivate future research in robust privacy-preserving learning for personal multimodal models.

REFERENCES

- [1] Martín Abadi, Andy Chu, Ian J. Goodfellow, and et al. 2016. Deep Learning with Differential Privacy. In *ACM Conference on Computer and Communications Security*.
- [2] Aishwarya Agrawal, Jiasen Lu, Stanislaw Antol, and et al. 2017. VQA: Visual Question Answering - www.visualqa.org. In *Int. J. Comput. Vis.*, Vol. 123. 4–31.
- [3] Jean-Baptiste Alayrac, Adrià Recasens, Rosalia Schneider, and et al. 2020. Self-Supervised MultiModal Versatile Networks. In *NeurIPS*.
- [4] Peter Anderson, Xiaodong He, Chris Buehler, and et al. 2018. Bottom-Up and Top-Down Attention for Image Captioning and Visual Question Answering. In *CVPR*.
- [5] Dzmitry Bahdanau, Kyunghyun Cho, and Yoshua Bengio. 2015. Neural Machine Translation by Jointly Learning to Align and Translate. In *ICLR*.
- [6] Christopher M Bishop. 2006. *Pattern recognition and machine learning*. Springer.
- [7] Ting Chen, Simon Kornblith, Mohammad Norouzi, and Geoffrey E. Hinton. 2020. A Simple Framework for Contrastive Learning of Visual Representations. In *ICML*.
- [8] Sumit Chopra, Raia Hadsell, and Yann LeCun. 2005. Learning a Similarity Metric Discriminatively, with Application to Face Verification. In *CVPR*.
- [9] Alec Radford et al. 2021. Learning Transferable Visual Models From Natural Language Supervision. In *ICML*.
- [10] Tianyu Gao, Adam Fisch, Danqi Chen, and et al. 2021. Making Pre-trained Language Models Better Few-shot Learners. In *ACL/IJCNLP*.
- [11] Yash Goyal, Tejas Khot, Aishwarya Agrawal, and et al. 2019. Making the V in VQA Matter: Elevating the Role of Image Understanding in Visual Question Answering. In *Int. J. Comput. Vis.*, Vol. 127. 398–414.
- [12] Chaoyang He, Zhengyu Yang, Erum Mushtaq, and et al. 2021. SSFL: Tackling Label Deficiency in Federated Learning via Personalized Self-Supervision.
- [13] Kaiming He, Haoqi Fan, Yuxin Wu, and et al. 2020. Momentum Contrast for Unsupervised Visual Representation Learning. In *CVPR*.
- [14] Briland Hitaj, Giuseppe Ateniese, and Fernando Pérez-Cruz. 2017. Deep Models Under the GAN: Information Leakage from Collaborative Deep Learning. In *CCS ACM*, 603–618.
- [15] Sepp Hochreiter and Jürgen Schmidhuber. 1997. Long Short-Term Memory. *Neural Comput.* 9, 8 (1997), 1735–1780.
- [16] Jin-Hwa Kim, Jaehyun Jun, Byoung-Tak Zhang, and et al. 2018. Bilinear Attention Networks. In *NeurIPS*.
- [17] Kyung-Min Kim, Min-Oh Heo, Seong-Ho Choi, and Byoung-Tak Zhang. 2017. DeepStory: Video Story QA by Deep Embedded Memory Networks. In *IJCAI*.
- [18] Seonhoo Kim, Seohyeong Jeong, Eunbyul Kim, Inho Kang, and Nojun Kwak. 2021. Self-supervised Pre-training and Contrastive Representation Learning for Multiple-choice Video QA. In *AAAI*.
- [19] Tae Kyun Kim. 2015. T test as a parametric statistic. In *Korean booktitle of anesthesiology*, Vol. 68.
- [20] Alex Krizhevsky, Ilya Sutskever, and Geoffrey E. Hinton. 2017. ImageNet classification with deep convolutional neural networks. *Commun. ACM* 60, 6 (2017), 84–90.
- [21] Daliang Li and Junpu Wang. 2019. FedMD: Heterogenous Federated Learning via Model Distillation.
- [22] Tsung-Yi Lin, Michael Maire, Serge J. Belongie, and et al. 2014. Microsoft COCO: Common Objects in Context. In *ECCV*.
- [23] Fenglin Liu, Xian Wu, Shen Ge, and et al. 2020. Federated Learning for Vision-and-Language Grounding Problems. In *AAAI*.
- [24] Yingqi Liu, Shiqing Ma, Yousra Aafer, and et al. 2018. Trojaning Attack on Neural Networks. In *Annual Network and Distributed System Security Symposium*.
- [25] Brendan McMahan, Eider Moore, Daniel Ramage, and et al. 2017. Communication-Efficient Learning of Deep Networks from Decentralized Data. In *AISTATS*.
- [26] Aaron Oord, Yazhe Li, Oriol Vinyals, and et al. 2018. Representation Learning with Contrastive Predictive Coding. In *arXiv Preprint*.
- [27] OpenAI. 2023. GPT-4 Technical Report. *CoRR abs/2303.08774* (2023).
- [28] Long Ouyang, Jeff Wu, Xu Jiang, and et al. 2022. Training language models to follow instructions with human feedback. *CoRR abs/2203.02155* (2022).
- [29] Mandela Patrick, Yuki Markus Asano, Ruth Fong, and et al. 2020. Multi-modal Self-Supervision from Generalized Data Transformations. In *arXiv preprint*.
- [30] Jeffrey Pennington, Richard Socher, Christopher D. Manning, and et al. 2014. GloVe: Global Vectors for Word Representation. In *EMNLP*.
- [31] Aditya Ramesh, Prafulla Dhariwal, Alex Nichol, and et al. 2022. Hierarchical Text-Conditional Image Generation with CLIP Latents. In *arXiv preprint arXiv:2204.06125*.
- [32] Aditya Ramesh, Mikhail Pavlov, Gabriel Goh, and et al. 2021. Zero-Shot Text-to-Image Generation. In *ICML*.
- [33] Andrew Rouditchenko, Angie W. Boggust, David Harwath, and et al. 2021. AVL-net: Learning Audio-Visual Language Representations from Instructional Videos. In *Annual Conference of the International Speech Communication Association*.
- [34] Yuwei Sun, Hideya Ochiai, and Hiroshi Esaki. 2020. Intrusion Detection with Segmented Federated Learning for Large-Scale Multiple LANs. In *IJCNN*.
- [35] Yuwei Sun, Hideya Ochiai, and Hiroshi Esaki. 2021. Decentralized Deep Learning for Multi-Access Edge Computing: A Survey on Communication Efficiency and Trustworthiness. In *IEEE Transactions on Artificial Intelligence*.
- [36] Chandra Thapa, M. A. P. Chamikara, Seyit Camtepe, and Lichao Sun. 2022. SplitFed: When Federated Learning Meets Split Learning. In *AAAI*.
- [37] Ashish Vaswani, Noam Shazeer, Niki Parmar, and et al. 2017. Attention is All you Need. In *NeurIPS*.
- [38] Ashish Vaswani, Noam Shazeer, Niki Parmar, and et al. 2017. Attention is All you Need. In *NeurIPS*.
- [39] Stefanie Warnat, Hartmut Schultze, Lingadahalli Shastry, and et al. 2021. Swarm Learning for decentralized and confidential clinical machine learning.
- [40] Zichao Yang, Xiaodong He, Jianfeng Gao, and et al. 2016. Stacked Attention Networks for Image Question Answering. In *CVPR*.
- [41] Zhou Yu, Yuhao Cui, Zhenwei Shao, Pengbing Gao, and Jun Yu. 2019. OpenVQA. <https://github.com/MLVLG/openvqa>.
- [42] Zhou Yu, Yuhao Cui, Jun Yu, and et al. 2020. Deep Multimodal Neural Architecture Search. In *ACM Multimedia*.
- [43] Zhou Yu, Jun Yu, Yuhao Cui, and et al. 2019. Deep Modular Co-Attention Networks for Visual Question Answering. In *CVPR*.
- [44] Zhou Yu, Jun Yu, Jianping Fan, and Dacheng Tao. 2017. Multi-modal Factorized Bilinear Pooling with Co-attention Learning for Visual Question Answering. In *ICCV*.
- [45] Jure Zbontar, Li Jing, Ishan Misra, and et al. 2021. Barlow Twins: Self-Supervised Learning via Redundancy Reduction.
- [46] Xi Zhu, Zhendong Mao, Chunxiao Liu, Peng Zhang, Bin Wang, and Yongdong Zhang. 2020. Overcoming Language Priors with Self-supervised Learning for Visual Question Answering. In *IJCAI*.

A APPENDICES

A.1 Attention Map Visualization

In Visual Question Answering (VQA), an attention mechanism [5, 38] is usually leveraged to learn to represent the relative importance of visual representations at different spatial locations with respect to a given question. The attention weights are updated such that the visual regions more relevant to the question are emphasized. Following [40], the attention maps were visualized in Fig. 7 by extracting the weight matrix from the learned attention mechanism.



Figure 7: The attention mechanism identifies the important regions that are relevant to answering the given question. These attention maps were generated by computing the weight matrix from the attention mechanism. The top image is about a question asking about the color of the sail, and the sail is highlighted. The bottom image is about a question asking about the number of dogs the man is walking, and the dogs are highlighted.

A.2 Computational Cost Estimation

The benefits for time reduction through the unidirectional architecture are demonstrated. Let the time cost of the forward propagation and the backpropagation for each component of split learning be $\{T_f^1, T_b^1\}$, $\{T_f^g, T_b^g\}$, and $\{T_f^2, T_b^2\}$. Then, the approximate total time cost for one epoch's training will be the sum of these values. Then, suppose that each component takes the same time to train in UniCon, then the approximate total time cost of it is $(\max(T_f^1, T_b^1) + T_f^g + T_b^g + \max(T_b^1, T_b^2))$. Therefore, the final reduced computational cost will be $(T_f^1 + T_b^1 + T_f^2 + T_b^2 - \max(T_f^1, T_b^1) - \max(T_b^1, T_b^2))$.

A.3 Algorithm

The detailed algorithm of Split Learning (without label sharing) is demonstrated in Algorithm 2.

Algorithm 2 Split Learning (without label sharing)

```

1:  $\theta_{\text{head},t}^{(k)}$ : parameters of  $f_{c,1}^{(k)}$ 
2:  $\theta_{\text{tail},t}^{(k)}$ : parameters of  $f_{c,2}^{(k)}$ 
3:  $G_t$ : parameters of  $f_g$ 
4:  $\delta_{g,e}$ : partial derivatives of  $f_g$  at local epoch  $e$ 
5:  $\delta_e^{(k)}$ : partial derivatives of  $f_{c,2}^{(k)}$  at local epoch  $e$ 
6:  $T$ : total training rounds
7:  $E$ : total local epochs
8:  $J$ : negative log likelihood loss
9:  $\eta$ : learning rate
10:  $D^{(k)} = (X^{(k)}, Y^{(k)})$ 
11: for each round  $t = 1, 2, \dots, T$  do
12:   for each client  $k \in \{1, 2, \dots, K\}$  in parallel do
13:      $G_t^{(k)} \leftarrow G_t$ 
14:      $\theta_{\text{head},t}^{(k)} \leftarrow \theta_{\text{head},t}$ 
15:      $\theta_{\text{tail},t}^{(k)} \leftarrow \theta_{\text{tail},t}$ 
16:     for each local epoch  $e = 1, 2, \dots, E$  do
17:        $v_e^{(k)} = f_{c,1}^{(k)}(\theta_{\text{head},t,e}^{(k)}, D^{(k)})$ 
18:        $v_e^g = \text{ServerForward}(v_e^{(k)}, G_{t,e}^{(k)})$ 
19:        $\delta_e^{(k)} = \frac{\partial J(f_{c,2}^{(k)}(\theta_{\text{tail},t,e}^{(k)}, v_e^g), Y^{(k)})}{\partial \theta_{\text{tail},t,e}^{(k)}}$ 
20:        $\theta_{\text{tail},t,e+1}^{(k)} \leftarrow \theta_{\text{tail},t,e}^{(k)} - \eta \cdot \delta_e^{(k)}$ 
21:        $\delta_{g,e}^{(k)}, G_{t,e+1}^{(k)} = \text{ServerBackprop}(\delta_e^{(k)}, G_{t,e}^{(k)})$ 
22:        $\theta_{\text{head},t,e+1}^{(k)} \leftarrow \theta_{\text{head},t,e}^{(k)} - \eta \cdot \frac{\partial \delta_{g,e}^{(k)}}{\partial \theta_{\text{head},t,e}^{(k)}}$ 
23:     end for
24:   end for
25:    $G_{t+1} = \frac{1}{K} \sum_{k \in K} G_{t,E+1}^{(k)}$ 
26:    $\theta_{\text{head},t+1} = \frac{1}{K} \sum_{k \in K} \theta_{\text{head},t,E+1}^{(k)}$ 
27:    $\theta_{\text{tail},t+1} = \frac{1}{K} \sum_{k \in K} \theta_{\text{tail},t,E+1}^{(k)}$ 
28: end for
29:
30: function ServerForward( $v_e^{(k)}, G_{t,e}^{(k)}$ )
31:  $v_e^g \leftarrow f_g(G_{t,e}^{(k)}, v_e^{(k)})$ 
32: return  $v_e^g$  to client
33:
34: function ServerBackprop( $\delta_e^{(k)}, G_{t,e}^{(k)}$ )
35:  $\delta_{g,e}^{(k)} = \frac{\partial \delta_e^{(k)}}{\partial G_{t,e}^{(k)}}$ 
36:  $G_{t,e+1}^{(k)} \leftarrow G_{t,e}^{(k)} - \eta \cdot \delta_{g,e}^{(k)}$ 
37: return  $\delta_{g,e}^{(k)}$  to client  $k$ 

```
